PHYSICAL REVIEW A **86**, 051606(R) (2012)

Fractional excitations in cold atomic gases

J. Honer,[1] J. C. Halimeh,[2] I. McCulloch,[3] U. Schollwöck,[2] and H. P. Büchler[1]
[1]*Institute for Theoretical Physics III, University of Stuttgart, Stuttgart, Germany*
[2]*Department of Physics and Arnold Sommerfeld Center for Theoretical Physics, Ludwig-Maximilians-Universität München, Munich, Germany*
[3]*Centre for Engineered Quantum Systems, School of Mathematics and Physics, University of Queensland, Brisbane 4072, Australia*
(Received 4 October 2012; published 27 November 2012)

We study the behavior of excitations in the tilted one-dimensional Bose-Hubbard model. In the phase with broken symmetry, fundamental excitations are domain walls which show fractional statistics. Using perturbation theory, we derive an analytic model for the time evolution of these fractional excitations, and demonstrate the existence of a repulsively bound state above a critical center-of-mass momentum. The validity of the perturbative analysis is confirmed by the use of time-adaptive density-matrix renormalization group simulations. These findings open the path for the experimental detection of fractional particles in cold atomic gases.

DOI: 10.1103/PhysRevA.86.051606 PACS number(s): 67.85.−d, 66.35.+a, 75.10.Pq

Excitations carrying fractional quantum numbers are one of the most intriguing features of strongly interacting many-body systems. Arguably the most celebrated of those is the charge $e/3$ Laughlin quasiparticle responsible for the fractional quantum Hall effect. Much effort is devoted to finding novel phases with even more exotic excitations such as non-Abelian anyons and fractional statistics in three-dimensional systems. In the quest for the experimental realization of such strongly correlated phases, cold atomic gases with their clean and controllable environment are a promising candidate and testing ground [1]. A first step in this direction marks the recently observed phase transition in a one-dimensional cold atomic system [2], where the fundamental excitations in the broken-symmetry phase are domain walls carrying an effective fractional charge. In this Rapid Communication, we investigate the creation and detection of these fractional excitations in the one-dimensional tilted Bose-Hubbard model.

A variety of theoretical proposals in cold atomic gases focus on the realization of strongly correlated phases with fractional excitations, such as models supporting spin-liquid phases [3], as well as Kitaev's toric code with Abelian anyonic excitations [4–6], and systems in large effective magnetic fields [7,8] exhibiting fractional quantum Hall states [9–15]. These proposals are based on standard experimental tools presently available in the context of quantum simulation (see Ref. [16] for a review). Especially, the latest development of experiments [17,18] with single-site readout and addressability in optical lattices has opened the path for the observation of a novel quantum phase transition in tilted optical lattices [2,19–21]. The transition in this one-dimensional system takes place from a phase with one atom on each lattice site, to a broken-symmetry phase (BSP) with an alternating mean occupation (see Fig. 1).

Here, we study the behavior of excitations in the tilted one-dimensional Bose-Hubbard model (TBH) in the phase with broken symmetry, with the latter being twofold degenerate. Fundamental excitations are domain walls between the degenerate broken-symmetry phases and exhibit an effective fractional charge. In turn, the simplest excitation corresponds to moving a single atom from one site to its neighboring site. Such an excitation corresponds to the creation of two closely bound domain walls. The important question is then whether these experimentally accessible excitations will decay into the fundamental domain-wall excitations and how to detect these fractional excitations. We derive an analytic expression for the time evolution of those excitations, and show the existence of a repulsively bound state of fractional excitations above a critical center-of-mass momentum $Q_c = 2\pi/3$. Further, we provide experimental signatures for measuring fractional excitations in a setup of cold atoms and give direct numerical calculations for the time evolution for a finite size sample.

We start with the one-dimensional tilted Bose-Hubbard model as realized in the experimental setup [17], which takes the form

$$H_{\mathrm{TBH}} = -w\sum_i (a_i^\dagger a_{i+1} + a_i a_{i+1}^\dagger) + \frac{U}{2}\sum_i n_i(n_i-1) - E\sum_i i n_i, \qquad (1)$$

with the on-site interaction U, the hopping rate w, and the lattice tilt E per site. In addition, $a_i^\dagger$ (a_i) is the creation (annihilation) operator for a particle on site i, and $n_i = a_i^\dagger a_i$ is the number operator on site i. We focus on the regime with an averaged density of one particle per lattice site, and assume a positive tilt $E > 0$, i.e., the lattice is tilted to the right. The system is in a metastable state, where the condition that the on-site interaction U and the lattice tilt E are much larger than the tunneling energy w prevents the relaxation into a state with more than two particles accumulating in a single site. Then, the relevant energies are the energy difference $\Delta = E - U$ and the hopping rate w.

For large negative Δ, the ground state is a Mott insulator (MI) with one particle per lattice site. Increasing $|\Delta| \sim w$, particles can tunnel to their right neighboring site, as long as the particle on that site has not tunneled. Eventually, the system undergoes a phase transition into a ground state with broken translational symmetry with two atoms on each second lattice site (see Fig. 1).

The condition $E, U \gg w, \Delta$ suppresses processes with particles hopping to the left as well as the accumulation of more than two particles in a single lattice site. These

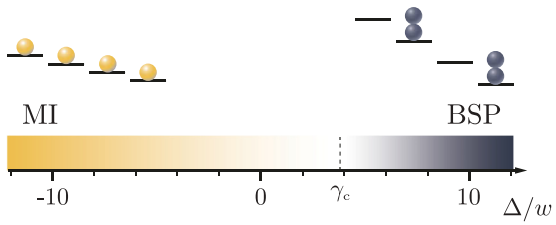

FIG. 1. (Color online) Phase diagram for the tilted Bose-Hubbard model in the regime $\Delta, w \ll U, E > 0$ and an averaged density of one particle per lattice site: The Mott insulator (MI) ground state for $\Delta/w < \gamma_c \approx 1.85$ [19], and the broken-symmetry phase (BSP) for $\Delta/w > \gamma_c$.

constraints are most conveniently incorporated by a mapping of the Bose-Hubbard model to a spin model: The spin degree of freedom resides between two lattice sites i and $i+1$ and the spin-up state corresponds to a particle at lattice site i, while the spin-down state accounts for the situation where the particle has tunneled to the site $i+1$. Then, the Bose-Hubbard model maps to a one-dimensional Ising model

$$H_{\text{Ising}} = -2\sqrt{2}w \sum_i S_x^i + \Delta \sum_i S_z^i + J \sum_i \left(S_z^i - \frac{1}{2}\right)\left(S_z^{i+1} - \frac{1}{2}\right), \tag{2}$$

where S_z^i (S_x^i) is the spin operator along the z (x) axis. In addition, the last term accounts for the constraint that a particle can only tunnel from site i to $i+1$ if there is already a particle at site $i+1$ and formally requires taking the limit $J \to \infty$. Under this mapping, the Mott-insulating state corresponds to a paramagnetic phase with all spin up, while the ordered broken-symmetry phase corresponds to an Ising antiferromagnetic ground state.

In the following, we focus on the quantum phase for $\Delta \gg w$ with two particles on every second lattice site. The experimentally accessible excitations are achieved by moving a particle from one lattice site to its neighboring site to the left, which corresponds to a single spin flip. The energy of this excitation is given by Δ. This single-particle excitation can now be decomposed into two fractional excitations via a second-order process, as indicated in Fig. 2. In the classical regime with $w = 0$, these delocalized fractional excitations have the same energy Δ as the single-spin excitations, while adding quantum fluctuations within second-order perturbation theory yields a nearest-neighbor interaction $V = 2w^2/\Delta$, as well as an effective hopping for the fractional excitations

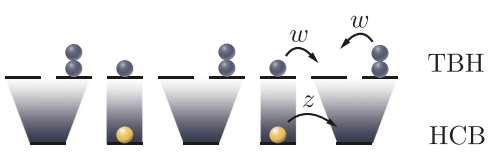

FIG. 2. (Color online) Mapping from the tilted Bose-Hubbard model (TBH) onto the effective hard-core boson model (HCB): Two neighboring lattice sites occupied by a 0,2 configuration map onto a single unoccupied site, whereas a singly occupied site maps onto an occupied site. A second-order transition with $2w^2/\Delta$ allows for an effective hopping of the fractional excitations.

with amplitude $z = 2w^2/\Delta$. Note that fractional excitations are restricted to even or odd lattice sites, depending on the local order, and hence hopping takes place from site i to site $i \pm 2$. This restriction can be uniquely fulfilled by introducing a new lattice: Each singly occupied site and the combination of a doubly occupied site next to an empty site count as a new lattice site (see Fig. 2). Consequently, the number of lattice sites between two excitations is halved, and the dynamics of fractional excitations is governed by the hard-core boson model (HCB) with nearest-neighbor hopping and interaction z and V, respectively, described by the Hamiltonian

$$H_{\text{HCB}} = -z \sum_j (b_j^\dagger b_{j+1} + b_j b_{j+1}^\dagger) + V \sum_j n_j n_{j+1}. \tag{3}$$

Here $b_j^\dagger$ (b_j) is the creation (annihilation) operator for a fractional excitation on site j, and $n_j = b_j^\dagger b_j$ is the number operator with $\langle n_j \rangle \in [0,1]$.

A similar Hamiltonian has previously been studied in the context of repulsively bound pairs [22,23]. Here, a bound state of domain walls means that the experimental excitation cannot decay into its fractional parts due to energy conservation, while the absence of a bound state corresponds to a situation where this experimental excitation decays into delocalized fractional excitations and allows for their experimental observation. As in the present situation, $z = V$ is the only energy scale of the model, we obtain a universal bound-state structure for the fractional excitations, which we analyze in the following.

We write the wave function for two fractional excitations in the effective model as $\psi(i,j)$, where i and j denote the positions of the fractional excitations in the effective lattice. The discrete translational invariance of the system provides conservation of the center-of-mass quasimomentum, which allows for an expansion into eigenfunctions of H_{HCB} for a fixed center-of-mass quasimomentum Q. Therefore, the two-particle wave function can be factorized as $\psi(X,x) = e^{-iQX}\psi(x)$, with the center of mass $X = (i+j)/2$ and relative coordinates $x = i - j$. We find two different regimes for the two-particle states: In the first regime for $|Q| \leqslant Q_c = 2\pi/3$, the two-particle eigenfunctions are given by scattering states ψ_q alone with energy $E_q = -2z_Q \cos q$, where q is the relative momentum and $z_Q = 2z \cos Q/2$ denotes the hopping rate in the center-of-mass frame. Its wave function reduces to plane waves, $\psi_q(x) = (1 - \delta_{x,0}) \cos(q|x| + \phi_{Q,q})$, with a scattering phase shift

$$\phi_{Q,q} = \arctan \frac{\cos q + 2 \cos Q/2}{\sin q}.$$

The Kronecker-delta factor $1 - \delta_{x,0}$ accounts for the hard-core constraint and enforces $\psi_q = 0$ at $x = 0$. In the second regime for $|Q| > Q_c$, an additional bound state ψ_B emerges. The repulsive interaction yields an energy $E_B = z(1 - 4\cos^2 Q/2)$ lying above the scattering continuum. Its two-particle wave function shows an exponential decay with relative distance x, and can be written as

$$\psi_B(x) = (1 - \delta_{x,0}) \left[\frac{1 - 4\cos^2 Q/2}{4\cos^2 Q/2}\right]^{\frac{1}{2}} \left(-2\cos\frac{Q}{2}\right)^{|x|}.$$

Note that the alternating amplitude of the wave function is a typical feature of a repulsively bound state. The general wave

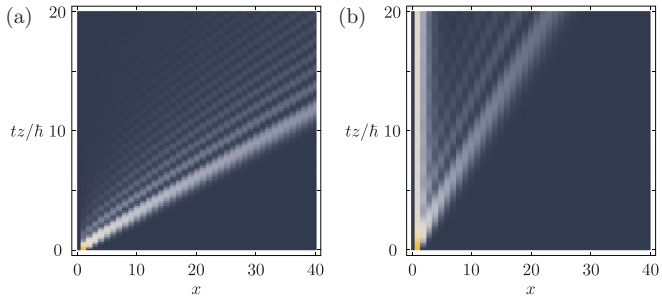

FIG. 3. (Color online) Time evolution of the relative wave function $\psi(x)$: (a) For $|Q| \leqslant Q_c$, the wave function is strongly localized at around a relative distance $x \sim tz_Q/\hbar$. (b) For $|Q| > Q_c$, the bound state adds an additional exponentially decaying contribution, with its maximum at $x = 1$.

function of two fractional excitations with a fixed center-of-mass momentum Q can therefore be decomposed as

$$\psi(x) = C_B \psi_B e^{-iE_B t/\hbar} + \int \frac{dq}{2\pi} C_q \psi_q e^{-iE_q t/\hbar}, \qquad (4)$$

with C_B and C_q denoting the overlap of the initial wave function with the bound and scattering eigenfunctions of H_{HCB}. The experimentally accessible initial states are achieved by moving one particle to the left, which in the effective model corresponds to two adjacent occupied sites $\psi_{SPE}(x) = \delta_{x,1}$. Then the overlap is given by $C_B = \theta(|Q| - Q_c)\sqrt{1 - 4\cos^2 Q/2}$ and $C_q = \sqrt{2}\cos(q + \phi_{Q,q})$, with $\theta(x)$ being the Heaviside step function. The integral over the relative quasimomentum q in Eq. (4) can be carried out analytically, giving rise to a formal solution in terms of an infinite sum of Bessel functions of the first kind,

$$\int \frac{dq}{2\pi} C_q \psi_q(x) e^{-iE_q t/\hbar} = \sum_n c_n(x) e^{i\frac{\pi}{2}n} J_n(2tz_Q/\hbar), \qquad (5)$$

with coefficients $c_n(x)$ defined via a discrete Fourier transform $C_q \psi_q(x) = \sum_n c_n(x) e^{iqn}$.

The time evolution of the wave function is shown in Fig. 3. The superposition of the scattering states leads to a ballistic expansion of the fractional excitations with a velocity determined by the hopping energy z_Q, i.e., the two-particle wave function ψ_{SPE} is strongly localized around a linearly growing relative distance $x \sim tz_Q/\hbar$, with some additional interference fringes appearing at smaller relative distances x, but propagating at the same velocity. However, the finite overlap with the bound state ψ_B for $Q > Q_c$ creates an additional stationary peak at $x \sim 1$ [see Fig. 3(b)]. With the scattering states moving away from each other, measurement of the wave-function amplitude at $x = 1$ at times $t \gg 1/z_Q$ allows one to single out the bound-state contribution. Formally, this can be cast in terms of a correlation function $C(t) = |\psi_{SPE}(X, x = 1)|^2$ on the effective lattice. In the microscopic lattice, $C(t)$ corresponds to $\langle P_i P_{i+1} \rangle$, with $P_i = n_i(n_i - 2)$ being the projection operator on singly occupied sites. The time evolution of $C(t)$ for different center-of-mass quasimomenta is shown in Fig. 4. For $Q < Q_c$, the correlation function decays to zero with a characteristic behavior $\sim(tz_Q/\hbar)^{-3}$, and exhibits characteristic oscillations due to interference between the different scattering states. In addition, the decay

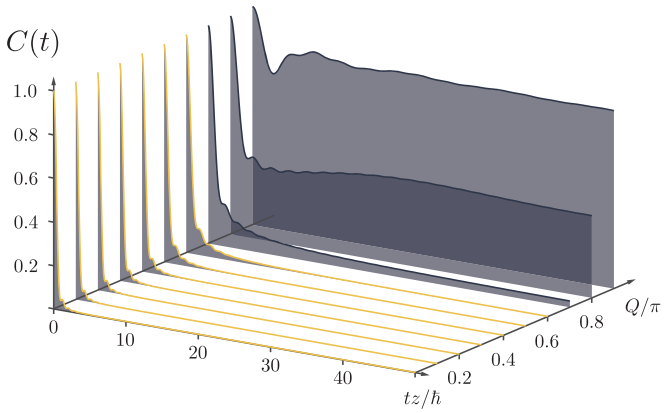

FIG. 4. (Color online) Time evolution of the correlation function $C(t)$ for different center-of-mass quasimomenta Q: Below the critical momentum $|Q| < Q_c$, the correlation function decays to zero, while for $|Q| > Q_c$ the overlap with the emerging repulsively bound state gives a finite probability for fractional excitations to stay at a finite relative distance x, resulting in a finite value of the correlation function for $tz_Q/\hbar \gg 1$.

exhibits an intermediate regime with a characteristic behavior $\sim(tz_Q/\hbar)^{-1}$. The time scale for the crossover between the long-time behavior and this intermediate regime diverges approaching the critical value Q_c. Consequently, the decay at $Q = Q_c$ is given by a critical behavior $\sim(tz_Q/\hbar)^{-1}$ for the correlation function, which follows from the analytical expression for the wave function

$$\psi_{SPE}(x) = e^{-i\frac{\pi}{2}|x|}[J_{|x|}(2zt) + iJ_{|x|-1}(2zt)].$$

Finally, the presence of a bound state is characterized by a saturation of the correlation function

$$C(t) \to \theta(|Q| - Q_c)[1 - 4\cos^2 Q/2]^2$$

for $tz_Q/\hbar \gg 1$. The bound-state contribution grows steadily towards the edge of the Brillouin zone, and eventually ψ_{SPE} becomes an eigenstate of the Hamiltonian at $|Q| = \pi$ with a constant correlation function $C(t) = 1$. In addition, the interference between the bound state and the scattering states gives rise to a characteristic beating of the correlation function with the frequencies $\omega^{\pm} = E_B \pm E_{SC}(q = 0) = z(1 - 4\cos^2 Q/2 \pm 2\cos Q/2)$. This gives experimental access to the energy gap between bound and scattering states, and allows for the measurement of the bound-state energy.

To confirm our perturbative results and to provide further insight into an experimental realization, we provide time-adaptive density matrix renormalization group (t-DMRG) simulations [24,25] of a single-particle excitation in the original tilted Bose-Hubbard model in Eq. (1). Here, we use a realistically large lattice of $L = 30$ sites, i.e., $l = 16$ sites in the effective lattice. Time-evolution calculations are performed using second- and fourth-order Trotter decompositions. A comparison between the analytic correlation function and the t-DMRG result is shown in Fig. 5.

On the one hand, t-DMRG results show good agreement with the perturbative model. We find that the time scale of the correlation-function decay and the saturation values agree well with the analytic results.

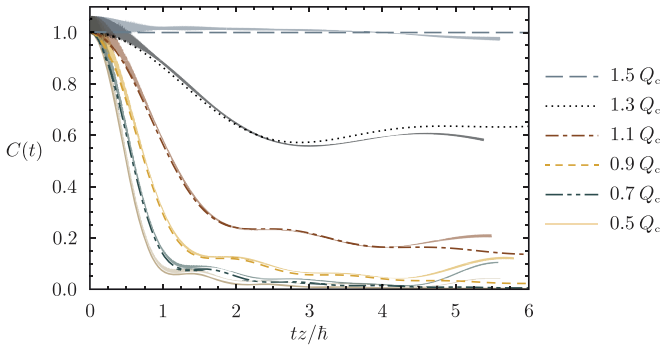

FIG. 5. (Color online) t-DMRG results (thin lines) in a finite lattice with $L = 30$ microscopic sites (i.e., $l = 16$ sites in the effective lattice) in comparison to the analytic results (thick lines) in an infinite lattice for center-of-mass momenta $Q/Q_c = 0.5$ (solid beige), 0.7 (dashed-double-dotted green), 0.9 (dashed yellow), 1.1 (dashed-dotted brown), 1.3 (dotted black), and 1.5 (long-dashed blue). Finite size effects start come into play at times $t \sim 4\hbar/z$.

On the other hand, we observe deviations due to finite system size and finite values U, E, and w, which we discuss in the following. First, the simulations are performed in a finite size system. This leads to revivals of the correlation function $C(t)$ due to scattering of fractional excitations at the system boundaries. In a microscopic lattice of $L = 30$ sites, we find deviations due to finite size at times $t \sim 4\hbar/z$. A hard-core model neglecting nearest-neighbor interaction, which allows for an analytic solution even in a finite system, agrees well with the t-DMRG result and gives an estimate for revival times. From this, we can derive a lower boundary of $L \gtrsim 26$ to observe a signature for a bound state in the correlation function. Second, the simulated correlation function shows an additional high-frequency oscillation. This can be explained as follows: Since the initial state is not an energy eigenstate of the Hamiltonian for a finite ratio w/Δ, this leads to interference between different energy contributions, and ultimately in oscillations on the order of the excitation spectrum, i.e., Δ. We find that for a ratio of $\Delta/w \gtrsim 30$ the suppression of these oscillations is strong enough to see a clear correlation-function signal (see Fig. 5).

Finally, the validity of the correlation function is based on the stability of the broken-symmetry phase. However, second-order processes in w/U and w/E allow the system to reach states with more than two particles on a single lattice site (see Ref. [19]). Our simulations show the probability for having three particles on a single lattice site at times $t = 4\hbar/z$ of the order 10^{-6}. It follows that this effect can be safely neglected for an on-site interaction $U \gtrsim 8\Delta$ on experimentally relevant time scales. With typical lifetimes of atoms in an optical lattice being on the order of seconds, an effective hopping rate $z/\hbar \sim 1$ Hz should be sufficient for observing the saturation of the correlation function $C(t)$. Further, assuming a microscopic hopping rate of $w = 15$ Hz, suppression of high-frequency oscillations yields a single-particle excitation energy $\Delta/\hbar = 450$ Hz. Finally, an on-site interaction $U/\hbar = 3.6$ kHz results in a stable broken-symmetry phase for the duration of the experiment.

An important aspect is that, throughout this Rapid Communication, calculations used an initial state of delocalized excitations with a finite center-of-mass momentum Q in order to maximize the correlation function $C(t)$. This behavior may seem counterintuitive, as one would expect a localized excitation to yield stronger correlations. However, localization in configuration space gives rise to a flat momentum distribution; with $C(t \gg \hbar/z) \to 0$ for $|Q| \leqslant Q_c$, this averaging over center-of-mass momenta then results in a decrease of the correlation function by a factor $\sim$0.17. Still, the finite-Q initial state can be composed of localized excitations via superposition, i.e.,

$$|\psi_Q\rangle = \sum_{j\in 2\mathbb{N}} e^{i\frac{Q}{2}j} a^\dagger_{j-1} a_j |\mathrm{BSP}\rangle, \tag{6}$$

with $|\mathrm{BSP}\rangle$ denoting the broken-symmetry phase with two particles on every even lattice site. The factor of 2 in the phase then accounts for the two-site hopping of fractional excitations in the microscopic model.

In conclusion, we have presented an experimentally accessible setup for studying the creation of fractional excitations. We have found that the stability of a single-particle excitation depends on its center-of-mass momentum, giving rise to a critical center-of-mass momentum $Q_c = 2\pi/3$. Furthermore, we have provided both analytical and numerical predictions on correlation functions, which are directly accessible at single-site resolution in optical lattices demonstrated recently by several groups [17,18].

We thank J. Simon and J. von Delft for fruitful discussions. Support from the DFG (Deutsche Forschungsgemeinschaft) within SFB/TRR21 and FOR 801 is acknowledged. I.McC. acknowledges support from the Australian Research Council Centre of Excellence for Engineered Quantum Systems and the Discovery Projects funding scheme (Project No. DP1092513). This research was supported in part by the National Science Foundation under Grant No. NSF PHY11-25915.

[1] M. Lewenstein *et al.*, Adv. Phys. **56**, 243 (2007).
[2] J. Simon *et al.*, Nature (London) **472**, 307 (2011).
[3] H. P. Büchler, M. Hermele, S. D. Huber, M. P. A. Fisher, and P. Zoller, Phys. Rev. Lett. **95**, 040402 (2005).
[4] A. Micheli, G. K. Brennen, and P. Zoller, Nat. Phys. **2**, 341 (2006).
[5] L.-M. Duan, E. Demler, and M. D. Lukin, Phys. Rev. Lett. **91**, 090402 (2003).
[6] Y.-J. Han, R. Raussendorf, and L.-M. Duan, Phys. Rev. Lett. **98**, 150404 (2007).
[7] J. Dalibard, F. Gerbier, G. Juzeliūnas, and P. Öhberg, Rev. Mod. Phys. **83**, 1523 (2011).
[8] D. Jaksch and P. Zoller, New J. Phys. **5**, 56 (2003).
[9] M. Roncaglia, M. Rizzi, and J. Dalibard, Sci. Rep. **1**, 43 (2011).
[10] R. N. Palmer and D. Jaksch, Phys. Rev. Lett. **96**, 180407 (2006).

[11] D. Sheng, Z.-C. Gu, K. Sun, and L. Sheng, Nat. Commun. **2**, 389 (2011).
[12] B. Juliá-Díaz, T. Graß, N. Barberán, and M. Lewenstein, New J. Phys. **14**, 055003 (2012).
[13] M. Popp, B. Paredes, and J. I. Cirac, Phys. Rev. A **70**, 053612 (2004).
[14] A. S. Sørensen, E. Demler, and M. D. Lukin, Phys. Rev. Lett. **94**, 086803 (2005).
[15] M. A. Baranov, K. Osterloh, and M. Lewenstein, Phys. Rev. Lett. **94**, 070404 (2005).
[16] I. Bloch, J. Dalibard, and S. Nascimbene, Nat. Phys. **8**, 267 (2012).
[17] W. S. Bakr, J. I. Gillen, A. Peng, S. Fölling, and M. Greiner, Nature (London) **462**, 74 (2009).
[18] J. F. Sherson *et al.*, Nature (London) **467**, 68 (2010).
[19] S. Sachdev, K. Sengupta, and S. M. Girvin, Phys. Rev. B **66**, 075128 (2002).
[20] M. Kolodrubetz, B. K. Clark, and D. A. Huse, Phys. Rev. Lett. **109**, 015701 (2012).
[21] S. Pielawa, T. Kitagawa, E. Berg, and S. Sachdev, Phys. Rev. B **83**, 205135 (2011).
[22] K. Winkler *et al.*, Nature (London) **441**, 853 (2006).
[23] Y.-M. Wang and J.-Q. Liang, Phys. Rev. A **81**, 045601 (2010).
[24] A. J. Daley, C. Kollath, U. Schollwöck, and G. Vidal, J. Stat. Mech.: Theory Exp. (2004) P04005.
[25] S. R. White and A. E. Feiguin, Phys. Rev. Lett. **93**, 076401 (2004).